IEEE Photonics Journal
An IEEE Photonics Society Publication

Open Access

Flexible and Concurrent All-Optical VPN in OFDMA PON

Volume 5, Number 6, December 2013

Xiaofeng Hu
Pan Cao
Liang Zhang
Xinhong Jiang
Zhiming Zhuang
Yikai Su, Senior Member, IEEE

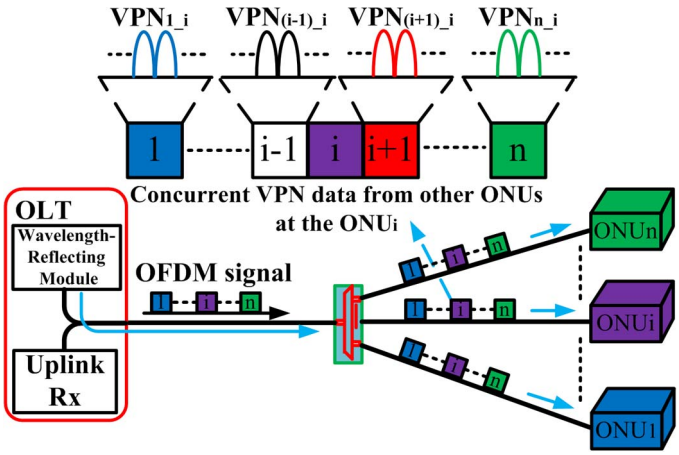

DOI: 10.1109/JPHOT.2013.2292300
1943-0655

IEEE photonics SOCIETY

IEEE

Flexible and Concurrent All-Optical VPN in OFDMA PON

Xiaofeng Hu, Pan Cao, Liang Zhang, Xinhong Jiang, Zhiming Zhuang, and Yikai Su, *Senior Member, IEEE*

State Key Laboratory of Advanced Optical Communication Systems and Networks, Department of Electronic Engineering, Shanghai Jiao Tong University, Shanghai 200240, China

DOI: 10.1109/JPHOT.2013.2292300

Manuscript received September 24, 2013; revised October 31, 2013; accepted November 2, 2013. Date of publication November 25, 2013; date of current version December 2, 2013. This work was supported in part by the National Natural Science Foundation of China under Grant 61125504 and in part by the 863 High-Tech Program under Grant 2013AA013402.

Abstract: We propose and experimentally demonstrate a new scheme to support an all-optical virtual private network (VPN) in orthogonal frequency-division multiple-access passive optical networks (OFDMA PONs). In our scheme, VPN communications among optical network units (ONUs) are concurrent, where each ONU can simultaneously transmit/receive different VPN traffic to/from other ONUs. Therefore, VPN communications between any two ONUs can be achieved at any time. The bit rates of VPN traffic can be also flexibly adjusted by using dynamic OFDM subcarrier-allocation technique. The proposed scheme is experimentally demonstrated with 5-Gb/s downlink, 2-Gb/s uplink, and 2-Gb/s VPN OFDM signals. Error-free performances are obtained for all these signals after 25-km standard single-mode fiber (SSMF) transmission.

Index Terms: Orthogonal frequency-division multiple access (OFDMA), passive optical network (PON), virtual private network (VPN).

1. Introduction

Fueled by an exponentially growing demand for various services, especially the bandwidth-intensive multimedia services, passive optical network (PON) has emerged as one of the most promising solutions for future-proof broadband access [1]–[3]. In a PON system, communications among end users are also becoming increasingly important in recent years owing to the development of pear-to-pear Internet applications, such as file sharing, cloud computing and interactive gaming [4]. All-optical virtual private network (VPN) is an effective approach to offer dedicated optical channels to connect end users, which reduces the latency of the network and provides enhanced security for customers [5]–[7]. Many efforts have been made to implement optical VPN communications in PON systems [8], [9]. In [8], radio-frequency (RF) subcarrier multiplexed transmission for intercommunications between end users is employed. In [9], a scheme of reconfigurable and scalable all-optical VPN in a wavelength division multiplexing (WDM) PON was proposed, which flexibly converted the VPN signal to different wavelengths based on cross-gain modulation (XGM) effect. However, in previous schemes, each optical network unit (ONU) can not deliver/receive different VPN data to/from other ONUs at the same time. In a practical network, the data of VPN communications among ONUs are usually not the same. In addition, the bit rates also need to be dynamically varied according to the VPN traffic requirements from end users. Thus the flexibility and concurrency of VPN communications among ONUs are desirable in next-generation access networks.

Recently, orthogonal frequency-division multiple-access (OFDMA) PON has been extensively studied since it features high spectral efficiency and superior tolerance against various fiber dispersion effects [10]–[12]. In an OFDMA PON, the overall bandwidth can be divided into multiple sub-bands in frequency domain. The optical line terminal (OLT) specifies the frequency-domain and time-domain resource allocations, and assigns each ONU multiple subcarriers in a given time slot according to the traffic requirements of ONUs. These characteristics are greatly beneficial to the implementation of flexible and concurrent VPN communications. In literatures, all-optical VPN in OFDMA PONs has been proposed, which however focused on realizing the intra- and inter-PON VPN communications and required high-precision comb optical filters at remote node to route different sub-bands of the OFDM signal [13].

In our previous work, an OFDMA PON architecture supporting variable-bit-rate VPN communications is reported [14]. Nonetheless, the scheme is relatively complicated and does not implement the concurrency of the VPN traffic. In this paper, we further propose and experimentally demonstrate a simple scheme to realize concurrent and flexible all-optical VPN in OFDMA PONs. The proposed scheme has several advantages. Firstly, the VPN communications are concurrent, i.e., each ONU can simultaneously transmit/receive different VPN data to/from other ONUs. Specially, each ONU can receive arbitrary VPN traffic from one or several or all other ONUs. Besides, the bit rates of VPN traffic can be dynamically varied to realize more flexible VPN communications by properly assigning the number of OFDM subcarriers. In our scheme, by using subcarrier allocation at each ONU, a combined 16-quadrature amplitude modulation (16-QAM) OFDM signal is generated, which consists of the uplink and concurrent VPN signals. Therefore, simultaneous transmission of uplink and concurrent VPN traffic is realized. At the OLT, a wavelength-reflecting module is used to reflect back the combined signals from ONUs. After detection, each ONU retrieves concurrent VPN data from the combined signals. The proposed scheme is experimentally demonstrated with 5-Gb/s downlink, 2-Gb/s uplink and 2-Gb/s VPN OFDM signals. Error-free performances are achieved for all these signals after transmission of 25-km standard single-mode fiber (SSMF).

2. Operation Principle

The schematic diagram of the proposed all-optical VPN in OFDMA PON is depicted in Fig. 1(a). At the OLT, a continuous wave (CW) light is launched into a Mach–Zehnder modulator (MZM). The MZM is biased at the quadrature point for linear electrical-to-optical (E/O) conversion and driven by the downlink electrical OFDM signal. After fiber transmission, the downlink signal is split by a 1:N splitter at remote node, and then routed to each ONU through different distribution fibers. At the ONU side, a waveband filter (WF) is employed to separate the downlink signal and the VPN signal simultaneously. The downlink signal is detected by a following downlink receiver. For the uplink and VPN traffic, another single-drive MZM at each ONU is biased at the quadrature point and driven by a combined electrical OFDM signal consisting of both the uplink and VPN data. After E/O conversion, the combined optical signal is delivered to the OLT through an optical circulator and 25-km optical fiber. At the OLT, the signals from ONUs are split into two parts using a 50:50 optical coupler. One part is directly detected by an uplink receiver to recover the uplink data from all ONUs, while the other part goes through a wavelength-reflecting module. The module reflects back all the combined signals to each ONU. After fiber transmission, the VPN signal is filtered by the WF and then detected by a VPN receiver at each ONU. It is noted that although the module might introduce additional cost, the cost can be shared by all ONUs in the network.

Fig. 1(b) describes the configuration of the combined OFDM signals delivered by the ONUs. According to the uplink and VPN traffic requirement, each ONU is allocated with a different sub-channel. The sub-channels of ONUs occupy different frequency bands. Block i $(i = 1, 2, \ldots, \mathrm{n})$ in Fig. 1(b) denotes the sub-channel assigned to $\mathrm{ONU_i}(i = 1, 2, \ldots, \mathrm{n})$. Taking $\mathrm{ONU_i}$ for instance, the bandwidth of the i-th sub-channel is further divided into multiple dedicated subcarrier groups for uplink signal and VPN communications with other ONUs. As depicted in the inset of Fig. 1(b), uplink data i represents the upstream data of $\mathrm{ONU_i}$, while $\mathrm{VPN_{i-k}}(k = 1, 2, \ldots, \mathrm{n}, k \neq i)$ represents the VPN data that $\mathrm{ONU_i}$ transmits to $\mathrm{ONU_k}(k = 1, 2, \ldots, \mathrm{n}, k \neq i)$. In this way, each ONU is capable of

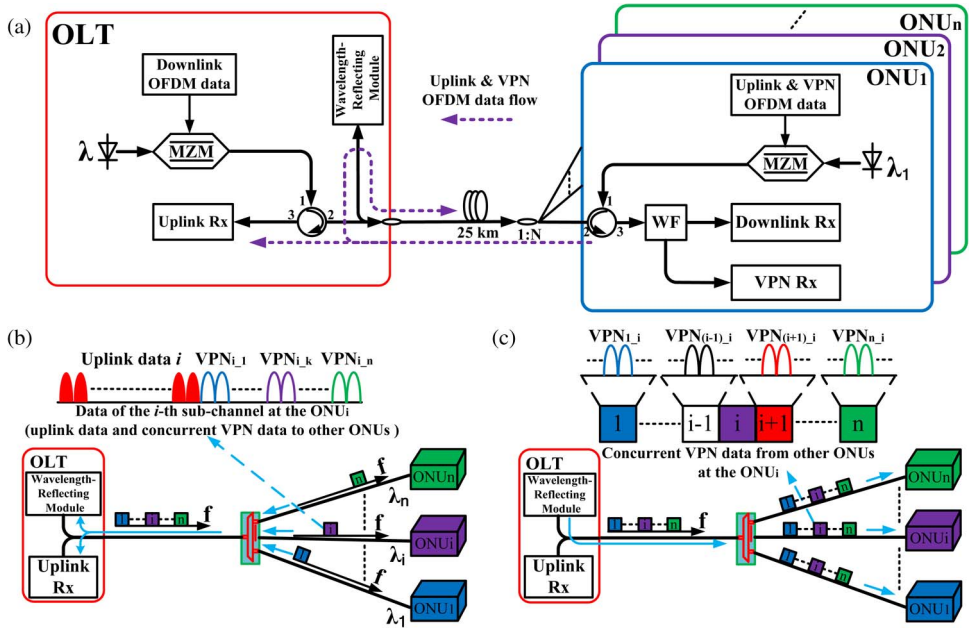

Fig. 1. (a) Schematic diagram of the proposed all-optical VPN in OFDMA PON (WF: waveband filter). (b) Combined uplink and VPN OFDM signal. (c) Received concurrent VPN OFDM signal.

delivering different VPN data to other ONUs in the same time slots. If there is no VPN communication between two ONUs at a certain time, the corresponding subcarriers could be re-allocated to the uplink traffic or other VPN traffic. Moreover, the number of subcarriers can be dynamically adjusted according to the traffic requirements of the uplink and VPN data from end users. Fig. 1(c) shows the reception of concurrent VPN OFDM signal at the ONU side. Each ONU receives the whole signal which consists of sub-channels for all VPN connections. For the reception of VPN data, ONU_i distinguishes and retrieves the subcarriers carrying VPN data from other ONUs to it as depicted in Fig. 1(c). With this method, each ONU is capable of receiving/transmitting VPN data from/to other ONUs at the same time. Compared with previous reports [5]–[9], [13], the flexibility and concurrency of all-optical VPN communications are achieved in our proposal.

3. Experimental Setup and Results

We perform a proof-of-concept experiment to verify the feasibility of the proposed all-optical VPN in OFDMA PON system as illustrated in Fig. 2. At the OLT, a 10-GHz single-drive MZM (JDSU OC-92) is utilized to modulate a CW light from a tunable laser (HP8168F) at 1558.32 nm. The MZM is biased at the quadrature point for linear E/O conversion and driven by the downlink electrical OFDM signal. The OFDM data is generated offline by Matlab. The total number of subcarriers is 1024. 16-QAM symbols are mapped onto the data subcarriers (256th $\sim$ 768th). In the data subcarriers, the 256th $\sim$ 383th & 641th $\sim$ 768th subcarriers are filled with downlink $data_3$ for ONU_3, while the 384th $\sim$ 640th subcarriers are loaded with downlink $data_4$ for ONU_4. A 1024-point IFFT with Hermitian symmetry [15], [16] is conducted to provide real numerical output data, and a cyclic prefix of 20 samples is added to alleviate the inter-symbol interference incurred by chromatic dispersion. The OFDM data is output by the arbitrary waveform generator (AWG_1) (Tektronix 7122C) at 5 GSample/s. Therefore, the OFDM signal has a bit rate of about 5 Gb/s, which can be simply obtained by the equation

$$C = \frac{n/2}{N + N_{cp}} \times Sa \times M \approx \frac{n/2}{N} \times Sa \times M \; Gb/s \tag{1}$$

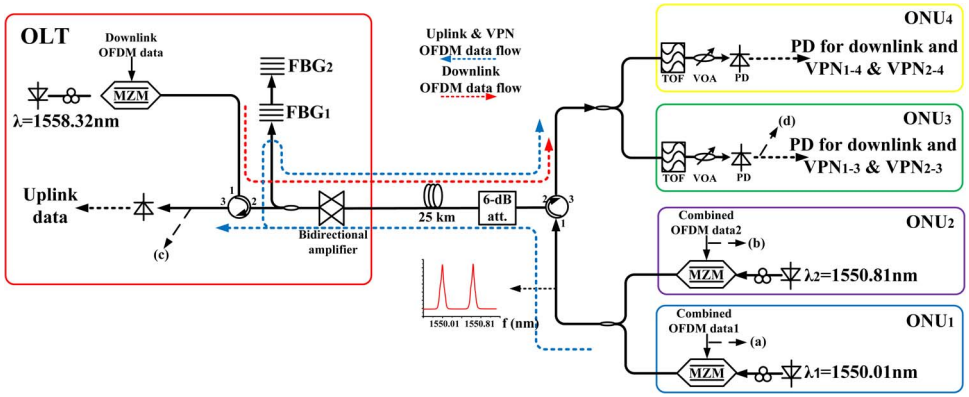

Fig. 2. Experimental setup of the proposed all-optical VPN in OFDMA PON. (a)–(d) Correspond to the electrical spectra shown in Fig. 3.

where n and N are the numbers of OFDM data subcarriers and IFFT points, N_{cp} is the cyclic prefix length, Sa is the sampling rate of AWG, and M is the number of bits per symbol. A bidirectional amplifier is used to compensate for the transmission loss. After amplification, the downlink signal is launched into a 25-km SSMF. At the ONU side, a 6-dB attenuator and a 50:50 coupler are added to emulate a 1:8 splitter (9-dB attenuation). At ONU_3 and ONU_4, a tunable optical filter (TOF) (Alnair BVF 200) is used to select the downlink OFDM signal, which is then detected by a 10-GHz photo detector (PD). A variable optical attenuator (VOA) is employed in each ONU to adjust the optical power of the received signal for measuring the bit error rate (BER) performance of OFDM signal as shown in Fig. 2.

For the uplink and VPN traffic, two CW lights from distributed feedback (DFB) lasers with wavelengths at λ_1 (1550.01 nm) and λ_2 (1550.81 nm) are injected into MZMs at ONU_1 and ONU_2, respectively. The MZMs at ONU_1 and ONU_2 are biased at the quadrature points and driven by the OFDM $data_1$ and $data_2$, respectively. The $data_1$ and $data_2$ are generated by AWG_2 (Tektronix 7122C) at 5 GSample/s, whose electrical spectra are provided in Fig. 3(a) and (b). At ONU_1, subcarriers (256th $\sim$ 355th & 669th $\sim$ 768th) are filled with $data_1$ with an IFFT size of 1024, while subcarriers (0th $\sim$ 255th & 356th $\sim$ 668th & 769th $\sim$ 1023th) are set to be zero as guard band. At ONU_2, subcarriers (406th $\sim$ 505th & 519th $\sim$ 618th) are loaded with $data_2$ with an IFFT size of 1024, while subcarriers (0th $\sim$ 405th & 506th $\sim$ 518th & 619th $\sim$ 1023th) are set to be zero. Therefore, both the combined $data_1$ and $data_2$ have a bit rate of $\sim$2 Gb/s. In our experiment, the configuration of the $data_1$ is the same as that of $data_2$. Taking the $data_1$ for instance, we assume that the 2-Gb/s combined signal consists of 1-Gb/s uplink $data_1$ (256th $\sim$ 305th & 719th $\sim$ 768th subcarriers) and 1-Gb/s VPN data (306th $\sim$ 355th & 669th $\sim$ 718th subcarriers). The VPN data includes VPN_{1-3} and VPN_{1-4}, which represent the data transmitted from ONU_1 to ONU_3 and ONU_4, respectively. Here, three cases are considered: 1) 1-Gb/s VPN_{1-3} data; 2) 0.7-Gb/s VPN_{1-3} data and 0.3-Gb/s VPN_{1-4} data; 3) 0.5-Gb/s VPN_{1-3} data and 0.5-Gb/s VPN_{1-4} data. We exploit dynamic OFDM subcarrier-allocation technique to implement the flexible VPN traffic among the ONUs. In case 1, there is no VPN communication between ONU_1 and ONU_4, and 100 subcarriers (306th $\sim$ 355th & 669th $\sim$ 718th) are all assigned to VPN_{1-3}. In case 2, the traffic demand of VPN_{1-3} communication becomes low, while that of VPN_{1-4} communication increases. 70 (306th $\sim$ 340th & 684th $\sim$ 718th) and 30 (341th $\sim$ 355th & 669th $\sim$ 683th) subcarriers are allocated to VPN_{1-3} and VPN_{1-4}, respectively. In case 3, the traffic requirements of VPN_{1-3} and VPN_{1-4} communications are similar. Both VPN_{1-3} and VPN_{1-4} are allocated with 50 subcarriers (306th $\sim$ 330th & 694th $\sim$ 718th and 331th $\sim$ 355th & 669th $\sim$ 693th). While there is no uplink traffic from ONUs, the maximum VPN bit rate among ONUs can achieve 10 Gb/s by using all 1024 subcarriers in our experiment.

After a 50:50 coupler, the $data_1$ and $data_2$ are combined to form an uplink & VPN signal, whose optical spectrum is shown in the inset of Fig. 2. An optical circulator at remote node is employed to direct the downlink signal and the uplink & VPN signal. At the OLT, the signal is divided into two

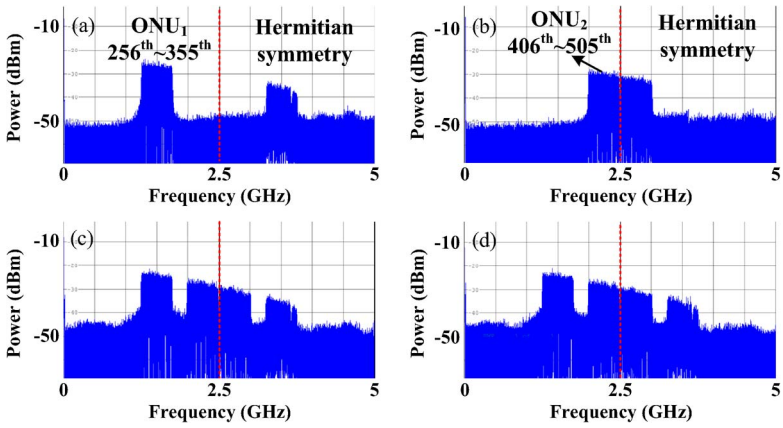

Fig. 3. Electrical spectra at different positions as indicated in Fig. 2. X-axis scale: 500 MHz/div (resolution bandwidth: 100 kHz). Y-axis scale: 10 dB/div. (a) Electrical combined OFDM data$_1$ at ONU$_1$, (b) electrical combined OFDM data$_2$ at ONU$_2$, (c) combined OFDM data after detection at the OLT, and (d) combined OFDM data after detection at ONU$_3$.

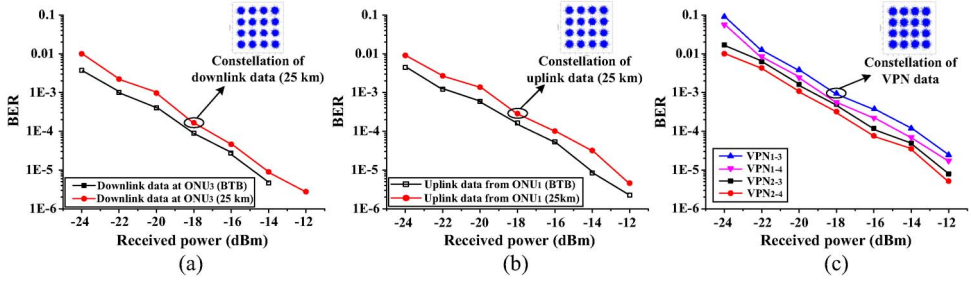

Fig. 4. BER curves and constellations of (a) downlink OFDM data, (b) uplink OFDM data, and (c) VPN$_{1-3}$ & VPN$_{2-3}$ and VPN$_{1-4}$ & VPN$_{2-4}$ in case 3.

parts by another 50:50 optical coupler. One part is directly detected by a 10-GHz PD to retrieve the uplink data from ONU$_1$ and ONU$_2$, whose electrical spectrum is provided in Fig. 3(c). With the increase of frequency, the power of OFDM subcarriers decreases as shown in Fig. 3(c), which mainly results from ~3.5-GHz 3-dB electrical bandwidth of AWG and beating noises generated by OFDM subcarriers. The other part goes through a wavelength-reflecting module, which consists of two cascading fiber Bragg gratings (FBGs). The two FBGs are utilized to reflect the combined signal to ONU$_3$ and ONU$_4$ (FBG$_1$: central wavelength at 1550.01 nm, 3-dB bandwidth of 0.104 nm, and reflection ratio of 90%; FBG$_2$: central wavelength at 1550.81 nm, 3-dB bandwidth of 0.106 nm, and reflection ratio of 90%). At the ONU side, the combined signal is separated from the downlink signal by the TOF. After detection by a 10-GHz PD, VPN$_{1-3}$ & VPN$_{2-3}$ and VPN$_{1-4}$ & VPN$_{2-4}$ data are selected and retrieved at ONU$_3$ and ONU$_4$, respectively. Fig. 3(d) shows the electrical spectrum after detection at ONU$_3$.

In our experiment, polarization controllers (PCs) are employed to maintain good modulation performances for MZMs. This limitation can be resolved by using commercially available polarization-insensitive modulators [17] or automatic polarizer stabilizers [18], [19]. After detection by the 10-GHz PD, the downlink OFDM signal and the combined OFDM signals are sampled by a Tektronix real-time oscilloscope (DSA 70804) with a sampling rate of 25 GSample/s. The downlink, uplink and VPN signals are processed and retrieved offline.

Fig. 4 shows the measured BER curves as a function of received power and corresponding constellations of the downlink, uplink and VPN OFDM data. For the downlink signal at ONU$_3$, the receiver sensitivity at a BER level of 2×10^{-3} (forward error correction threshold) is -23.7 dBm in the back-to-back (BTB) case and 1.3-dB power penalty is observed after 25-km fiber transmission.

For the uplink signal from ONU_1, the receiver sensitivities are −23.2 dBm and −22.1 dBm in the case of BTB and 25-km fiber transmission, respectively. The sensitivity penalty caused by the fiber transmission is about 1.1 dB for the uplink transmission.

The BER curves of VPN data in all the three cases show small differences. Fig. 4(c) depicts the BER curves of VPN_{1-3} & VPN_{2-3} and VPN_{1-4} & VPN_{2-4} data in case 3. The receiver sensitivities of VPN_{1-3}, VPN_{1-4}, VPN_{2-3} and VPN_{2-4} data are −19.8 dBm, −20.3 dBm, −20.9 dBm, and −21.5 dBm, respectively. The differences of receiver sensitivity for VPN data are mainly attributed to the frequency response of the AWG. In addition, the performances of devices at ONU_1 and ONU_2 also contribute to the differences. The insets in Fig. 4(a)–(c) show the corresponding constellations of the downlink, uplink and VPN signal, respectively. It is worth noting that the Rayleigh backscattering (RB) noise would become an important issue for the all-optical VPN communications in the OFDMA PON with a high split ratio [20], [21]. However, a wavelength-shifting module can be introduced at the OLT to mitigate the RB noise as proposed in our previous work [14].

4. Conclusion

We have proposed and demonstrated an OFDMA PON architecture, which provides flexible and concurrent all-optical VPN communications. In our scheme, concurrent VPN communications among ONUs are achieved and the bit rates of concurrent VPN traffic are varied by OFDM subcarrier-allocation technique. A proof-of-concept experiment is carried out to verify the feasibility of the proposal. Successful transmissions of 5-Gb/s downlink, 2-Gb/s uplink and 2-G/s VPN 16-QAM OFDM signals over 25-km SSMF are implemented. Experimental results show that our scheme could be a promising solution to realize flexible and concurrent communications of all-optical VPN in OFDMA PON.

References

[1] J. Kani, F. Bourgart, A. Cui, A. Rafel, and S. Rodrigues, "Next-generation PON—Part I: Technology roadmap and general requirements," *IEEE Commun. Mag.*, vol. 47, no. 11, pp. 43–49, Nov. 2009.

[2] F. J. Effenberger, H. Mukai, S. Park, and T. Pfeiffer, "Next-generation PON—Part II: Candidate systems for next-generation PON," *IEEE Commun. Mag.*, vol. 47, no. 11, pp. 50–57, Nov. 2009.

[3] G. Kramer and G. Pesavento, "Ethernet passive optical network (EPON): Building a next-generation optical access network," *IEEE Commun. Mag.*, vol. 40, no. 2, pp. 66–73, Feb. 2002.

[4] Y. Su, Y. Tian, E. Wong, N. Nadarajah, and C. Chan, "All-optical virtual private network in passive optical networks," *Laser Photon. Rev.*, vol. 2, no. 6, pp. 460–479, Dec. 2008.

[5] R. Cohen, "On the establishment of an access VPN in broadband access networks," *IEEE Commun. Mag.*, vol. 41, no. 2, pp. 156–163, Feb. 2003.

[6] Y. Tian, X. Tian, L. Leng, T. Ye, and Y. Su, "Optical VPN connecting ONUs in different PONs," presented at the Opt. Fiber Commun. Conf., Anaheim, CA, USA, 2007, Paper OWL6.

[7] Q. Zhao and C. Chan, "A wavelength-division-multiplexed passive optical network with flexible optical network unit Internetworking capability," *J. Lightw. Technol.*, vol. 25, no. 8, pp. 1970–1977, Aug. 2007.

[8] N. Nadarajah, M. Attygalle, E. Wong, and A. Nirmalathas, "Novel schemes for local area network emulation in passive optical networks with RF subcarrier multiplexed customer traffic," *J. Lightw. Technol.*, vol. 23, no. 10, pp. 2974–2983, Oct. 2005.

[9] X. Hu, L. Zhang, P. Cao, G. Zhou, F. Li, and Y. Su, "Reconfigurable and scalable all-optical VPN in WDM PON," *IEEE Photon. Technol. Lett.*, vol. 23, no. 14, pp. 941–943, Jul. 2011.

[10] J. L. Wei, C. Sánchez, R. P. Giddings, E. Hugues-Salas, and J. M. Tang, "Significant improvements in optical power budgets of real-time optical OFDM PON systems," *Opt. Exp.*, vol. 18, no. 20, pp. 20 732–20 745, Sep. 2010.

[11] D. Qian, J. Hu, P. N. Ji, T. Wang, and M. Cvijetic, "10-Gb/s OFDMA-PON for delivery for heterogeneous services," presented at the Opt. Fiber Commun. Conf., San Diego, CA, USA, 2008, Paper OWH4.

[12] Y. M. Li, "Demonstration and design of high spectral efficiency 4 Gb/s OFDM system in passive optical networks," presented at the Opt. Fiber Commun. Conf., Anaheim, CA, USA, 2007, Paper OThD7.

[13] C. Zhang, J. Huang, C. Chen, and K. Qiu, "All-optical virtual private network and ONUs communication in optical OFDM-based PON system," *Opt. Exp.*, vol. 19, no. 24, pp. 24 816–24 821, Nov. 2011.

[14] Z. Zhuang, M. Xu, J. Wu, P. Cao, X. Hu, T. Wang, and Y. Su, "An OFDMA-PON architecture supporting flexible all-optical VPN with source-free ONUs," presented at the Photon. Global Conf., Singapore, 2012, Paper 3-4B-6.

[15] B. Schmidt, A. Lowery, and J. Armstrong, "Experimental demonstrations of electronic dispersion compensation for long-haul transmission using direct-detection optical OFDM," *J. Lightw. Technol.*, vol. 26, no. 1, pp. 196–203, Jan. 2008.

[16] B. Schmidt, A. Lowery, and J. Armstrong, "Experimental demonstrations of 20 Gbit/s direct-detection optical OFDM and 12 Gbit/s with a colorless transmitter," presented at the Opt. Fiber Commun. Conf., Anaheim, CA, USA, 2007, Paper PDP18.

[17] N. Cvijetic, D. Qian, J. Hu, and T. Wang, "44-Gb/s/λ upstream OFDMA-PON transmission with polarization-insensitive source-free ONUs," presented at the Opt. Fiber Commun. Conf., San Diego, CA, USA, 2010, Paper OTuO2.
[18] J. Perez, M. Morant, R. Llorente, and J. Martí, "Joint distribution of polarization-multiplexed UWB and WiMAX radio in PON," *J. Lightw. Technol.*, vol. 27, no. 12, pp. 1912–1919, Jun. 2009.
[19] "Reset-free polarization stabilizer—polastay," in *General Photonics*. [Online]. Available: http://www.generalphotonics.com/pdf/ PolaStay.pdf
[20] C. Arellano, K. Langer, and J. Prat, "Reflections and multiple Rayleigh backscattering in WDM single-fiber loopback access networks," *J. Lightw. Technol.*, vol. 27, no. 1, pp. 12–18, Jan. 2009.
[21] J. Wei, E. Hugues-Salas, R. Giddings, X. Jin, X. Zheng, S. Mansoor, and J. Tang, "Wavelength reused bidirectional transmission of adaptively modulated optical OFDM signals in WDM-PONs incorporating SOA and RSOA intensity modulators," *Opt. Exp.*, vol. 18, no. 10, pp. 9791–9808, May 2010.